Redox Chemistry

Deutsche Ausgabe: DOI: 10.1002/ange.201603659
Internationale Ausgabe: DOI: 10.1002/anie.201603659

Redox-Active-Ligand-Mediated Formation of an Acyclic Trinuclear Ruthenium Complex with Bridging Nitrido Ligands

*Bidraha Bagh, Daniël L. J. Broere, Maxime A. Siegler, and Jarl Ivar van der Vlugt**

Abstract: *Coordination of a redox-active pyridine aminophenol ligand to Ru^{II} followed by aerobic oxidation generates two diamagnetic Ru^{III} species [**1a** (cis) and **1b** (trans)] with ligand-centered radicals. The reaction of **1a**/**1b** with excess NaN_3 under inert atmosphere resulted in the formation of a rare bis(nitrido)-bridged trinuclear ruthenium complex with two nonlinear asymmetrical Ru-N-Ru fragments. The spontaneous reduction of the ligand centered radical in the parent **1a**/**1b** supports the oxidation of a nitride (N^{3-}) to half an equivalent of N_2. The trinuclear omplex is reactive toward TEMPO-H, tin hydrides, thiols, and dihydrogen.*

The preparation and reactivity of late-transition-metal nitrides has attracted much attention as metal–nitrogen multiple bonds become increasingly more difficult to accommodate with high-electron-count d-metal ions.[1] Group 8 metal nitrides have enjoyed specific attention because of their relevance as faithful nitrogenase model systems.[2] Both terminal[3] (**I**–**III**; Figure 1) and bridging[4] (**IV**–**VI**) ruthenium nitrido complexes have been reported for Ru^{IV}, Ru^{V}, and Ru^{VI} oxidation states.[5] Terminal Ru≡N species are highly electrophilic and reactive toward a variety of substrates, and involve inter alia H_2 activation and hydrogen atom transfer (HAT) reactions.[6] These mechanisms allow, for example, hydrogenolysis (to NH_3) or radical-type bond functionalization. In contrast, the reactivity of ruthenium complexes with bridging nitrido ligands is unexplored. Furthermore, multinuclear ruthenium complexes with nonlinear and asymmetrically bridging nitrido ligands are extremely rare.[7]

Redox-active ligands have emerged as a very appealing class of ligands to induce odd-electron chemistry on either redox-inert or platinum-group metal complexes.[8] Aminophenol-derived architectures have been particularly forthcoming in allowing new reactivity for a variety of transition metals, for example, by either acting as an electron reservoir to enable two-electron chemistry at d^0 metal centers or invoking radical reactivity in the coordination sphere of noble metals.[9] Ruthenium complexes with redox-active

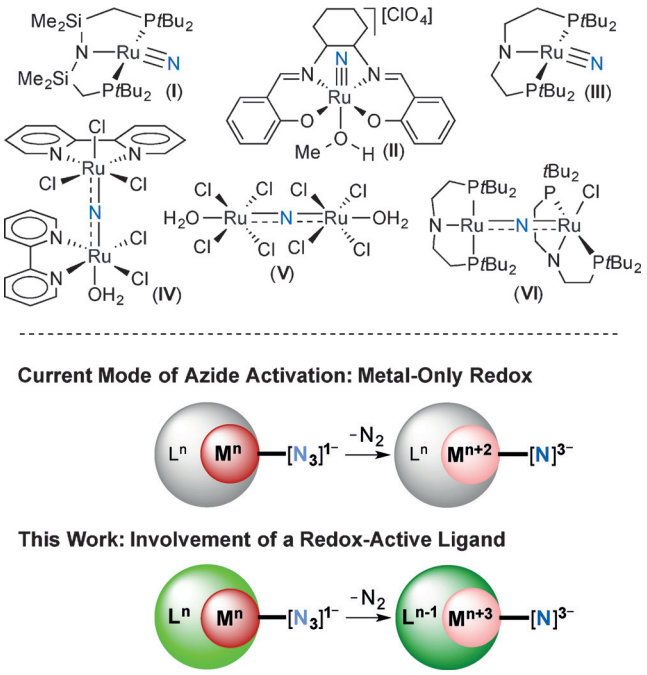

Figure 1. Top: Representative terminal (**I**–**III**) and bridging (**IV**–**VI**) ruthenium-nitrido species. Bottom: Azide decomposition without (upper) and with (lower) involvement of a redox-active ligand mediating oxidation state of a late-transition metal.

catecholato and *o*-amidophenolato systems are well-known.[10] However, the potential for intramolecular redox chemistry between ruthenium nitrido species and redox-active ligands is uncharted. Such electron-transfer phenomena might significantly impact the resulting reactivity (as well as provide a potential route toward generation) of such nitrido species. We herein address a synthetic strategy to manipulate azido-to-nitrido conversion by introducing electronic interplay between a redox-active ligand motif and a ruthenium center, which induces a higher metal oxidation state. This strategy has allowed the isolation of a unique trinuclear species bearing a highly asymmetric Ru-N-Ru-N-Ru skeleton featuring one redox-active ligand per ruthenium. Preliminary reactivity screening suggests that the resulting bridging nitride fragments are susceptible to hydrogen-atom transfer from TEMPO-H, tin hydrides, thiols, and activation of dihydrogen.

We previously reported the synthesis, electrochemistry, and (catalytic) reactivity of square-planar palladium(II) complexes bearing a redox-active pyridine aminophenol ligand $\mathbf{NNO^{H2}}$ and close analogues thereof (Scheme 1).[11] Coordination of $\mathbf{NNO^{H2}}$ to $[RuCl_2(PPh_3)_3]$ under inert

[*] Dr. B. Bagh, D. L. J. Broere, Dr. Ir. J. I. van der Vlugt
Homogeneous, Bioinspired and Supramolecular Catalysis
Van't Hoff Institute for Molecular Sciences, University of Amsterdam
Science Park 904, 1098 XH, Amsterdam (The Netherlands)
E-mail: j.i.vandervlugt@uva.nl
Dr. M. A. Siegler
Small Molecule X-ray Crystallography Facility
Department of Chemistry, John Hopkins University
Baltimore, MD 21218 (USA)

Supporting information for this article can be found under: http://dx.doi.org/10.1002/anie.201603659.

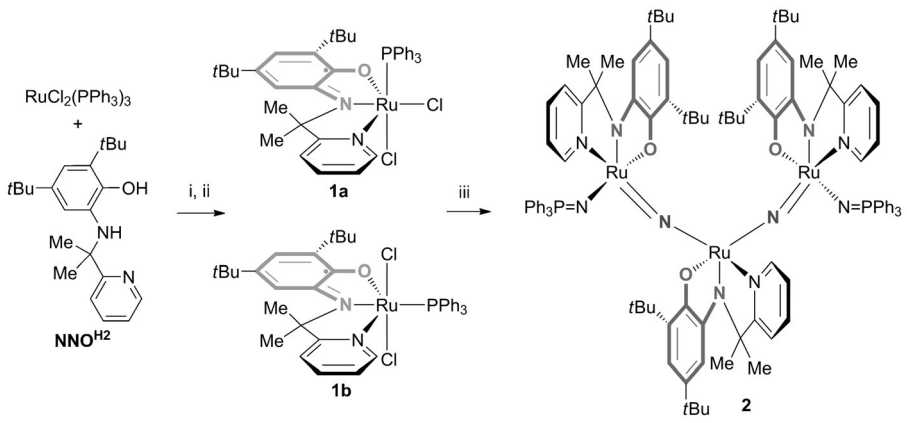

Scheme 1. Synthesis of **1a**, **1b**, and **2**: 1) 1 molar equiv $[RuCl_2(PPh_3)_3]$, C_6H_6, Ar, 24 h; 2) air, 48 h; 3) excess NaN_3, THF, Ar, 48 h. THF = tetrahydrofuran.

The reaction of **1a** in THF with excess NaN_3 for two days under inert atmosphere and ambient light conditions resulted in the selective formation of the dark-brown complex **2** (Scheme 1). The IR spectrum of this species does not contain any stretch attributable to an azido fragment. Exclusion of light had no effect on the outcome of the reaction and using **1b** under identical reaction conditions led to the same result. Species **2** is diamagnetic and shows C_1 symmetry on the NMR timescale. The ^{31}P NMR spectrum showed two resonances at $\delta = 22.69$ and 26.34 ppm in C_6D_6. Slow diffusion of *n*-pentane into a benzene solution of **2** afforded single crystals suitable for X-ray structure determination (Figure 3). The Ru–O,

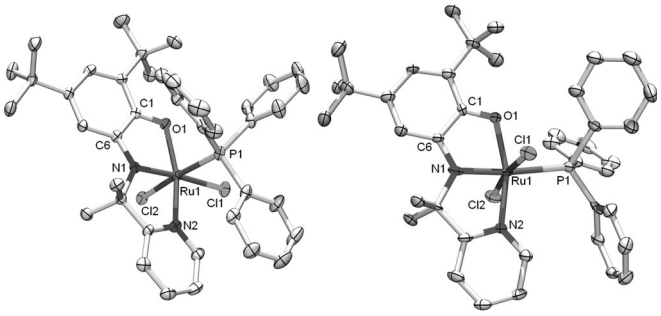

Figure 2. Displacement ellipsoid plots (50% probability level) of **1a** and **1b** (H atoms and lattice solvent molecules (for **1b**) omitted for clarity).[23] Selected bond lengths [Å] and angles [°]: For **1a**: Ru1-O1 2.063(2), Ru1-N1 1.904(2), C1-O1 1.283(4), C6-N1 1.349(4), C1-C6 1.443(4); Cl1-Ru1-Cl2 88.01(3). For **1b**: Ru1-O1 2.040(4), Ru1-N1 1.907(6), C1-O1 1.283(8), C6-N1 1.357(8), C1-C6 1.453(9); Cl1-Ru1-Cl2 170.93(7).

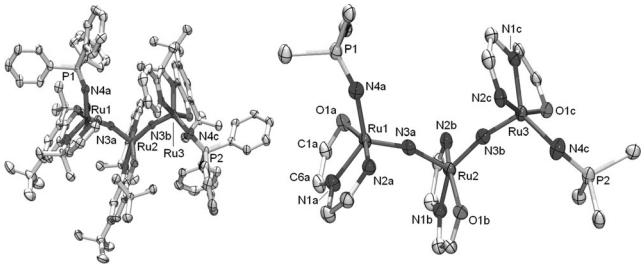

Figure 3. Left: displacement ellipsoid plots (50% probability level) of **2** (H atoms and lattice solvent molecules are omitted for clarity). Right: View of core skeleton of **2**.[23] Selected bond lengths [Å] and angles [°]: Ru1-O1a 2.018(3), Ru2-O1b 1.992(3), Ru3-O1c 2.017(3), Ru1-N1a 1.907(3), Ru2-N1b 1.945(2), Ru3-N1c 1.928(3), Ru1-N3a 1.694(3), Ru3-N3b 1.695(3), Ru2-N3a 1.844(3), Ru2-N3b 1.871(3); Ru1-N3a-Ru2 162.14(2), Ru2-N3b-Ru3 166.74(2), N3a-Ru2-N3b 96.84(1), N2a-Ru1-N3a 96.44(13), N3a-Ru1-N4a 113.92(15), P1-N4a-Ru1 137.0(2), P2-N4c-Ru3 131.7(2).

atmosphere followed by aerobic oxidation resulted in two species, identified as *cis*-$[RuCl_2(PPh_3)(\mathbf{NNO})]$ (**1a**) and *trans*-$[RuCl_2(PPh_3)(\mathbf{NNO})]$ (**1b**), in a roughly equimolar ratio based on multinuclear NMR spectroscopy. These isomers were isolated as dark-violet (**1a**, 43%) and dark-blue (**1b**, 46%) diamagnetic crystalline solids. The NMR spectra of **1b** are consistent with overall C_s symmetry, while **1a** exhibits C_1 symmetry on the NMR timescale. The molecular structures of **1a** and **1b** were confirmed by single-crystal X-ray diffraction (Figure 2). The geometry around the ruthenium centers in **1a** and **1b** is distorted octahedral, and the ruthenium–ligand bond lengths are comparable.[12,13]

By using the metric oxidation state (MOS) method,[14] values of $-0.74(\pm 0.07)$ and $-0.78(\pm 0.14)$ were obtained for **1a** and **1b**, respectively.[15] Based on the observed non-integer MOS values and the interaction between the DFT calculated ligand orbital with a metal π-type orbital (see the Supporting Information), we prefer an intermediate description between $Ru^{II}/\mathbf{NNO^{IBQ}}$ and $Ru^{III}/\mathbf{NNO^{ISQ}}$ rather than a pure $Ru^{III}/\mathbf{NNO^{ISQ}}$ situation for **1a** and **1b**, with antiferromagnetic coupling between Ru^{III} and $\mathbf{NNO^{ISQ}}$ likely accounting for the overall diamagnetic character of these species (see the Supporting Information).

Ru–N, and $Ru–N_{pyr}$ bond lengths are similar at the three ruthenium centers. Also both phosphiniminato ($N{=}PPh_3$) moieties show comparable $Ru–N_P$ bond lengths, but their relative opposing orientation with respect to the NNO framework of the central ruthenium makes these $Ru–N{=}PPh_3$ units magnetically inequivalent. The $Ru–N_{nitrido}$ bonds with the peripheral Ru centers [1.694(3) and 1.695(3) Å] are much shorter than the $Ru–N_{nitrido}$ bonds with the central Ru center [1.871(3) and 1.844(3) Å]. The Ru-N-Ru fragments deviate significantly from linearity [∠Ru-N-Ru of 162.14(2) and 166.74(2)] relative to known nitrido-bridged dinuclear ruthenium complexes.[4] These combined data suggest that Ru=N–Ru–N=Ru is an appropriate description for the bonding description in **2**.

Metal nitrido species are commonly generated by photolysis or thermolysis of the corresponding metal azido complexes, although salt metathesis of ruthenium halides with, for example, NaN_3 sometimes leads to the spontaneous forma-

tion of nitrido species without detection of the relevant azido intermediate.[3a,4d] We set out to investigate the mechanism of the reaction of **1** with NaN_3 to generate **2**. Reaction of **1a** with excess NaN_3 in [D_8]THF was monitored by ^{1}H and ^{31}P NMR spectroscopy (Figure 4; for **1b** see the Supporting Information).

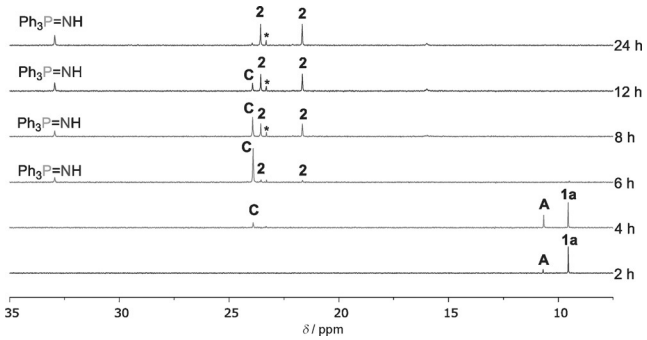

Figure 4. Progress of the reaction of **1a** with NaN_3 in [D_8]THF monitored by ^{31}P NMR spectroscopy (Ph_3PO is indicated by *).

Based on the experimental data and supported by DFT (see the Supporting Information), we propose the following mechanism for the formation of **2** from **1a** (Scheme 2). Initial chloride substitution of **1a** by sodium azide yields the bis(azido) complex **A** within four hours, with a visible color change from dark-violet to dark-green and appearance of a strong IR band at 2027 cm^{-1}.[16,17] After 6 hours, concomitant with a color change from dark-green to dark-blue, a new major species was observed by ^{1}H and ^{31}P NMR spectroscopy (see the Supporting Information). This species **C** is formulated as a ruthenium nitrido complex, [Ru(N)(N=PPh_3)(**NNO**)], bearing a phosphiniminato moiety, with strong IR bands at 1041 (Ru≡N) and 1092 cm^{-1} (N=P).[18] Trapping of **C** with PPh_3 gave the [Ru(N=PPh_3)$_2$(**NNO**)] **3**, which was spectroscopically characterized. Ultimately, three molecules of **C** combine to form the trinuclear complex **2** within 24 hours, concomitant with the elimination of formally half an equivalent of dinitrogen and one equivalent of iminophosphorane (Ph_3P=NH), which was detected by ^{31}P NMR spectroscopy ($\delta = 32.94$)[19] and mass spectrometry [m/z 277 (M^+)].

Based on the metric parameters obtained experimentally from X-ray crystallography, all three NNO moieties are best described as fully reduced amidophenolato **NNO^{AP}** fragments [MOS values of −1.98(±0.10), −1.81(±0.06) and −1.77(±0.09)].[14,15] The metric parameters were well-reproduced by the DFT optimized geometry. Analysis of the molecular orbitals revealed highly delocalized orbitals over the Ru-N-Ru-N-Ru skeleton, including the highest occupied molecular orbital (HOMO; Figure 5). The spin density of the optimized geometry in the triplet state, which is higher in energy by 16.0 kcal mol^{-1}, showed similar delocalization. The large singlet–triplet gap is indicative of strong anti-ferromagnetic coupling. Consequently, we propose to describe the electronic structure of **2** as [(L)(**NNO^{AP}**)Ru^V]-N^{3-}-[Ru^{IV}(**NNO^{AP}**)]-N^{3-}-[Ru^V(**NNO^{AP}**)(L)] (L = N=PPh_3) with highly delocalized anti-ferromagnetically coupled electrons over the Ru-N-Ru-N-Ru framework.

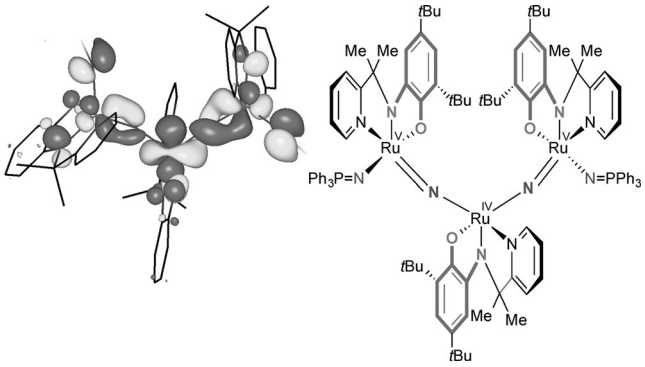

Figure 5. Left: DFT (BP86, def2-TZVP) calculated HOMO of the optimized geometry of **2**. Right: proposed predominant redox-isomer of **2**.

The structural data of **2** suggest three dianionic amidophenolato **NNO^{AP}** states, which supports intramolecular substrate-to-ligand electron transfer, thus resulting in one-electron reduction of each ligand and three-electron reduction overall, relative to the starting complex **1**, upon reaction with azide. This corresponds to the oxidation of a nitrido ligand (N^{3-}) to half an equivalent of N_2 (Scheme 3). The formation of N_2 is supported by mass spectrometry when **1a**

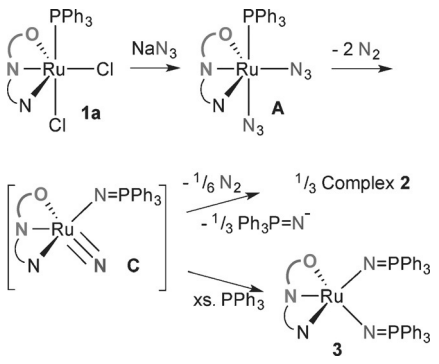

Scheme 2. Proposed pathway for reaction of **1a** toward NaN_3 with formation of **2** via the intermediates **A** and **C**, and trapping of **C** to generate **3**.

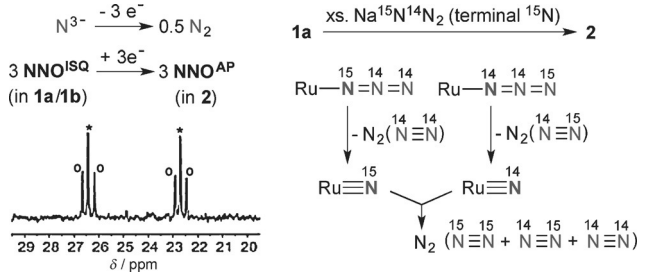

Scheme 3. Isotopic-labelling experiment showing the formation of three isotopomers of N_2 and ^{31}P NMR spectrum of isotopomers of complex **2**. * represents ^{14}N isotopomer, ° indicates ^{15}N isotopomer.

was reacted with $Na^{15}N^{14}N_2$ (terminal ^{15}N) in THF under argon for two days in a closed vessel. The nitride and phosphiniminato of **C** contain both ^{14}N (50%) and ^{15}N (50%). Dinitrogen formed from azide activation would give only $^{14}N^{14}N$ and $^{15}N^{14}N$. Mass analysis of the headspace above the reaction medium revealed the additional presence of $^{15}N^{15}N$, which supports the reductive coupling of two ruthenium nitrides toward N_2.[20] The corresponding ^{15}N-labeled isotopomer of **2** resulted in two new doublets in the ^{31}P NMR spectrum.

When **2** is exposed to 5 bar of H_2 at 50°C, two new ^{31}P resonances at $\delta = 17.65$ (broad) and 38.00 ppm (sharp) were obtained within 12 hours (see the Supporting Information for details). A pure dark-brown diamagnetic solid, correlating to the sharp singlet at $\delta = 38.00$ ppm, precipitated out of solution upon cooling. Variable-temperature ^1H NMR spectroscopy showed resonances for three chemically inequivalent **NNO** ligands and one coordinated $N{=}PPh_3$ moiety. Mass analysis (m/z 1626.54 $[M]^+$) supported formulation of this species, **4**, as [(L)(**NNO**)Ru]-NH-[Ru(**NNO**)]-NH-[Ru(**NNO**)] (L = $N{=}PPh_3$). A weak, broad IR band was present at 3576 cm^{-1}, which can be attributed to a bridging NH moiety.[21] We have no indication for the formation of a Ru–H species during the course of the reaction (monitored by ^1H NMR spectroscopy). The same spectroscopic features were obtained upon reaction of **2** with 2 equivalents of TEMPO-H in $[D_8]$THF, with the TEMPO$^\bullet$ radical being detected by EPR spectroscopy. The reaction of **2** with 2 equivalents of either PhSH or BuSnH as hydrogen-atom donors also led to **4**, and PhS–SPh and BuSn–SnBu, respectively. Although it is reasonable to assume that both H_2 activation and hydrogen atom transfer occur directly at the bridging nitrido fragments, an alternative pathway involving short-lived Ru–H species cannot be fully excluded. Additional studies to elucidate the detailed mechanism for these HAT reactions are ongoing.

In conclusion, ruthenium complexes **1a** and **1b**, which are best described as ruthenium(III) species with a ligand-centered **NNO^{ISQ}** radical, undergo spontaneous azide decomposition upon salt metathesis with NaN_3 to generate a rare trinuclear ruthenium complex (**2**) featuring two asymmetric Ru-N-Ru fragments. The redox-active **NNO** ligands appear to act as electron acceptors, thus facilitating the formation of the trinuclear assembly and N_2. Isotopic labeling supports nitride coupling as the source of dinitrogen. The high extent of delocalization over the Ru-N-Ru-N-Ru fragment is a possible explanation for the observed diamagnetism. The bridging nitride moieties in **2** displays hydrogen-atom transfer reactivity towards TEMPO-H, tin hydride, and thiol. Similarly **2** reacts with H_2 and thus might be catalytically competent for hydrogen-transfer reactions.[22]

Acknowledgments

Research funded by the European Research Council (ERC) through Starting Grant 279097 to J.I.v.d.V. We thank Ed Zuidinga for ESI-MS, Norbert Geels for MS analysis of N_2 isotopomers and Professors Bas de Bruin and Joost Reek for general discussions.

Keywords: azides · density functional calculations · redox chemistry · ruthenium · structure determination

How to cite: *Angew. Chem. Int. Ed.* **2016**, *55*, 8381–8385
Angew. Chem. **2016**, *128*, 8521–8525

[1] a) J. F. Berry, *Comments Inorg. Chem.* **2009**, *30*, 28–66; b) K. Ray, F. Heims, F. F. Pfaff, *Eur. J. Inorg. Chem.* **2013**, 3784–3807; c) V. Vreeken, M. A. Siegler, B. de Bruin, J. N. H. Reek, M. Lutz, J. I. van der Vlugt, *Angew. Chem. Int. Ed.* **2015**, *54*, 7055–7059; *Angew. Chem.* **2015**, *127*, 7161–7165.

[2] Recent reviews: a) W.-L. Man, W. W. Y. Lam, T.-C. Lau, *Acc. Chem. Res.* **2014**, *47*, 427–439; b) X.-Y. Yi, Y. Liang, C. Li, *RSC Adv.* **2013**, *3*, 3477–3486; group 8 complexes: c) S. D. Brown, J. C. Peters, *J. Am. Chem. Soc.* **2005**, *127*, 1913–1923; d) J. J. Scepaniak, J. A. Young, R. P. Bontchev, J. M. Smith, *Angew. Chem. Int. Ed.* **2009**, *48*, 3158–3160; *Angew. Chem.* **2009**, *121*, 3204–3206; e) J. J. Scepaniak, R. P. Bontchev, D. L. Johnson, J. M. Smith, *Angew. Chem. Int. Ed.* **2011**, *50*, 6630–6633; *Angew. Chem.* **2011**, *123*, 6760–6763; f) J. J. Scepaniak, C. S. Vogel, M. M. Khusniyarov, F. W. Heinemann, K. Meyer, J. M. Smith, *Science* **2011**, *331*, 1049–1052; g) J. Hohenberger, K. Ray, K. Meyer, *Nat. Commun.* **2012**, *3*, 1–13; h) T. M. Powers, T. A. Betley, *J. Am. Chem. Soc.* **2013**, *135*, 12289–12296; i) A. I. Olivos Suarez, V. Lyaskovskyy, J. N. H. Reek, J. I. van der Vlugt, B. de Bruin, *Angew. Chem. Int. Ed.* **2013**, *52*, 12510–12529; *Angew. Chem.* **2013**, *125*, 12740–12760.

[3] a) L. Bonomo, E. Solari, R. Scopelliti, C. Floriani, *Angew. Chem. Int. Ed.* **2001**, *40*, 2529–2531; *Angew. Chem.* **2001**, *113*, 2597–2599; b) W.-L. Man, T.-M. Tang, T.-W. Wong, T.-C. Lau, S.-M. Peng, W.-T. Wong, *J. Am. Chem. Soc.* **2004**, *126*, 478–479; c) A. Walstrom, M. Pink, X. Yang, J. Tomaszewski, M.-H. Baik, K. G. Caulton, *J. Am. Chem. Soc.* **2005**, *127*, 5330–5331; d) W.-L. Man, J. Xie, P.-K. Lo, W. W. Y. Lam, S.-M. Yiu, K.-C. Lau, T.-C. Lau, *Angew. Chem. Int. Ed.* **2014**, *53*, 8463–8466; *Angew. Chem.* **2014**, *126*, 8603–8606.

[4] a) W. P. Griffith, N. T. McManus, A. C. Skapski, *J. Chem. Soc. Chem. Commun.* **1984**, 434–435; b) M. Haukka, T. Venaldinen, M. Ahlgrén, T. A. Pakkanen, *Inorg. Chem.* **1995**, *34*, 2931–2936; c) T. Jüstel, J. Bendix, N. Metzler-Nolte, T. Weyhermüller, B. Nuber, K. Wieghardt, *Inorg. Chem.* **1998**, *37*, 35–43; d) S. Matsumura, K. Shikano, T. Oi, N. Suzuki, H. Nagao, *Inorg. Chem.* **2008**, *47*, 9125–9127; e) O. Halevi, B. Bogoslavsky, D. Grinstein, F. Tibika-Apfelbaum, A. Bino, *Inorg. Chim. Acta* **2014**, *421*, 228–232; f) A. Glüer, B. Askevold, B. Schluschaß, F. W. Heinemann, S. Schneider, *Z. Anorg. Allg. Chem.* **2015**, *641*, 49–51.

[5] Nitrido-bridged multinuclear ruthenium clusters are also known: a) J. P. Attard, B. F. G. Johnson, J. Lewis, J. M. Mace, P. R. Raithby, *J. Chem. Soc. Chem. Commun.* **1985**, 1526–1528; b) C. E. Anson, J. P. Attard, B. F. G. Johnson, J. Lewis, J. M. Mace, D. B. Powell, *J. Chem. Soc. Chem. Commun.* **1986**, 1715–1717; c) S. Harris, M. L. Blohm, W. L. Gladfelter, *Inorg. Chem.* **1989**, *28*, 2290–2297.

[6] a) W.-L. Man, W. W. Y. Lam, H.-K. Kwong, S.-M. Peng, W.-T. Wong, T.-C. Lau, *Inorg. Chem.* **2010**, *49*, 73–81; b) B. Askevold, J. T. Nieto, S. Tussupbayev, M. Diefenbach, E. Herdtweck, M. C. Holthausen, S. Schneider, *Nat. Chem.* **2011**, *3*, 532–537; c) S. Abbina, S. Bian, C. Oian, G. Du, *ACS Catal.* **2013**, *3*, 678–684.

[7] W.-M. Cheung, E. K. Huang, J. Zhu, X.-Y. Yi, H. H. Y. Sung, I. D. Williams, W.-H. Leung, *Inorg. Chem.* **2013**, *52*, 10449–10455.

[8] a) O. R. Luca, R. H. Crabtree, *Chem. Soc. Rev.* **2013**, *42*, 1440–1459; b) V. K. K. Praneeth, M. R. Ringenberg, T. R. Ward, *Angew. Chem. Int. Ed.* **2012**, *51*, 10228–10234; *Angew. Chem.* **2012**, *124*, 10374–10380; c) V. Lyaskovskyy, B. de Bruin, *ACS Catal.* **2012**, *2*, 270–279.

[9] D. L. J. Broere, R. Plessius, J. I. van der Vlugt, *Chem. Soc. Rev.* **2015**, *44*, 6886 – 6915.
[10] a) K. Kobayashi, H. Ohtsu, T. Wada, T. Kato, K. Tanaka, *J. Am. Chem. Soc.* **2003**, *125*, 6729 – 6739; b) Y. Miyazato, T. Wada, J. T. Muckerman, E. Fujita, K. Tanaka, *Angew. Chem. Int. Ed.* **2007**, *46*, 5728 – 5730; *Angew. Chem.* **2007**, *119*, 5830 – 5832; c) A. K. Das, B. Sarkar, C. Duboc, S. Strobel, J. Fiedler, S. ZáliŠ, G. K. Lahiri, W. Kaim, *Angew. Chem. Int. Ed.* **2009**, *48*, 4242 – 4245; *Angew. Chem.* **2009**, *121*, 4306 – 4309; d) J. D. Ingram, P. J. Costa, H. Adams, M. D. Ward, V. Félix, J. A. Thomas, *Inorg. Chem.* **2012**, *51*, 10483 – 10494; e) M. Bubrin, D. Schweinfurth, F. Ehret, S. Zális, H. Kvapilová, J. Fiedler, Q. Zeng, F. Hartl, W. Kaim, *Organometallics* **2014**, *33*, 4973 – 4985.
[11] a) D. L. J. Broere, B. de Bruin, J. N. H. Reek, M. Lutz, S. Dechert, J. I. van der Vlugt, *J. Am. Chem. Soc.* **2014**, *136*, 11574 – 11577; b) D. L. J. Broere, L. L. Metz, B. de Bruin, J. N. H. Reek, M. A. Siegler, J. I. van der Vlugt, *Angew. Chem. Int. Ed.* **2015**, *54*, 1516 – 1520; *Angew. Chem.* **2015**, *127*, 1536 – 1540; c) D. L. J. Broere, S. Demeshko, B. de Bruin, M. A. Siegler, F. Hartl, J. I. van der Vlugt, *Chem. Eur. J.* **2015**, *21*, 5879 – 5886; d) D. L. J. Broere, D. K. Modder, E. Blokker, M. A. Siegler, J. I. van der Vlugt, *Angew. Chem. Int. Ed.* **2016**, *55*, 2406 – 2410; *Angew. Chem.* **2016**, *128*, 2452 – 2456.
[12] J. L. Boyer, J. Rochford, M. K. Tsai, J. T. Muckerman, E. Fujita, *Coord. Chem. Rev.* **2010**, *254*, 309 – 330.
[13] S. Bhattacharya, P. Gupta, F. Basuli, C. G. Pierpont, *Inorg. Chem.* **2002**, *41*, 5810 – 5816.
[14] S. N. Brown, *Inorg. Chem.* **2012**, *51*, 1251 – 1260.
[15] See also Ref. [13]. Some computational studies suggest that formal oxidation state assignments based on crystallographic data may not necessarily be very accurate for ruthenium complexes with redox-active *o*-aminophenol-derived ligands: a) C. Remenyi, M. Kaupp, *J. Am. Chem. Soc.* **2005**, *127*, 11399 – 11413; b) G. Skara, B. Pinter, P. Geerlings, F. De Proft, *Chem. Sci.* **2015**, *6*, 4109 – 4117; c) G. Skara, M. Gimferrer, F. De Proft, P. Salvador, B. Pinter, *Inorg. Chem.* **2016**, *55*, 2185 – 2199.
[16] a) C.-W. Chang, G.-H. Lee, *Organometallics* **2003**, *22*, 3107 – 3116; b) K. S. Singh, K. A. Kreisel, G. P. A. Yap, M. R. Kollipara, *J. Organomet. Chem.* **2006**, *691*, 3509 – 3518; c) Y.-H. Lo, T.-H. Wang, C.-Y. Lee, Y.-H. Feng, *Organometallics* **2012**, *31*, 6887 – 6899; d) S. Miguel-Fernández, S. M. de Salinas, J. Díez, M. P. Gamasa, E. Lastra, *Inorg. Chem.* **2013**, *52*, 4293 – 4302.
[17] Starting from *trans*-**1b** also produced **2**. However, the initial species **B** (the analogue of **A**) showed a singlet for the geminal Me groups, whereas for **A** the diastereotopic Me groups appear as two singlets, thus supporting initial *trans* versus *cis* orientation of both N_3 ligands.
[18] See Ref. [2g] and: a) P.-M. Chan, W.-Y. Yu, C.-M. Che, K.-K. Cheung, *J. Chem. Soc. Dalton Trans.* **1998**, 3183 – 3190; b) A. R. Corcos, A. K. M. Long, I. A. Guzei, J. F. Berry, *Eur. J. Inorg. Chem.* **2013**, 3808 – 3811.
[19] J. A. Reisz, E. B. Klorig, M. W. Wright, S. B. King, *Org. Lett.* **2009**, *11*, 2719 – 2721. The source of hydrogen required to generate free iminophosphorane is likely the bulk solvent.
[20] a) M. G. Scheibel, B. Askevold, F. W. Heinemann, E. J. Reijerse, B. de Bruin, S. Schneider, *Nat. Chem.* **2012**, *4*, 552 – 558; b) Y. Gloaguen, C. Rebreyend, M. Lutz, P. Kumar, M. Huber, J. I. van der Vlugt, S. Schneider, B. de Bruin, *Angew. Chem. Int. Ed.* **2014**, *53*, 6814 – 6818; *Angew. Chem.* **2014**, *126*, 6932 – 6936.
[21] a) D. J. Knobloch, E. Lobkovsky, P. J. Chirik, *J. Am. Chem. Soc.* **2010**, *132*, 10553 – 10564; b) S. P. Semproni, E. Lobkovsky, P. J. Chirik, *J. Am. Chem. Soc.* **2011**, *133*, 10406 – 10409; c) Y. Lee, F. T. Sloane, G. Blondin, K. A. Abboud, R. García-Serres, L. J. Murray, *Angew. Chem. Int. Ed.* **2015**, *54*, 1499 – 1503; *Angew. Chem.* **2015**, *127*, 1519 – 1523.
[22] Preliminary experiments show efficient hydrogenation of terminal alkenes (1-hexene and 1-octene) at 5 bar H_2 and 50 °C with 1 mol % **2**.
[23] CCDC 1474188 (**1a**), 1474187 (**1b**), and 1474190 (**2**) contain the supplementary crystallographic data for this paper. These data can be obtained free of charge from The Cambridge Crystallographic Data Centre.

Received: April 14, 2016
Published online: June 20, 2016

